Boundary-integral method for poloidal axisymmetric AC magnetic fields

J. Priede and Gunter Gerbeth

***Abstract*— This paper presents a boundary-integral equation (BIE) method for the calculation of poloidal axisymmetric magnetic fields applicable in a wide range of ac frequencies. The method is based on the vector potential formulation and it uses the Green's functions of Laplace and Helmholtz equations for the exterior and interior of conductors, respectively. The work is particularly focused on a calculation of axisymmetric Green's function for the Helmholtz equation which is both simpler and more accurate compared to previous approaches. Three different approaches are used for calculation of the Green's function depending on the parameter range. For low and high dimensionless ac frequencies we use a power series expansion in terms of elliptical integrals and an asymptotic series in terms of modified Bessel functions of second kind, respectively. For the intermediate frequency range, Gauss-Chebyshev-Lobatto quadratures are used. The method is verified by comparing with the analytical solution for a sphere in a uniform external ac field. The application of the method is demonstrated for a composite model inductor containing an external secondary circuit.**

***Index Terms*— Integral equations, Green function, Helmholtz equations, Boundary-element method, Electrical engineering computing**

I. Introduction

CALCULATION of alternating magnetic fields and the associated eddy currents is important for the design of various electrical machines and the magnetic field inductors used for heating, melting, stirring, shaping or levitation of metallic or semiconducting materials. Although the distribution of electromagnetic fields is, in principle, completely described by the Maxwell equations, only in very few simple cases these equations can be solved analytically. Usually a numerical approach is needed.

Most of the approaches used for the solution of electromagnetic field problems are based on finite difference (FDM) or finite element methods (FEM). The main advantage of these methods is their capability to deal with complex geometrical configurations usually encountered in practical applications. However, these methods involve a solution for the fields in the free space which is often unbounded and, thus, may require considerable additional computer resources as well as a special numerical treatment at the outer open boundary [1].

Manuscript received April 28, 2004; revised October 27, 2005. This work was supported by Deutsche Forschungsgemeinschaft in frame of the Collaborative Research Centre SFB 609 and by the European Commission under grant No. G1MA-CT-2002-04046.

J. Priede was with Forschungszentrum Rossendorf, P.O. Box 510119, 01314 Dresden, Germany during this work. Presently he is with the Institute of Physics, University of Latvia, Miera st. 32, LV–2169 Salaspils, Latvia;

G. Gerbeth is with Forschungszentrum Rossendorf, MHD Department, P.O. Box 510119, 01314 Dresden, Germany

On the other hand, in many applications such as, for example, electromagnetic heating and hardening of workpieces or the stirring of molten metals, only the eddy currents and magnetic fields in the conducting medium are needed. There are several approaches avoiding the solution of the magnetic field in the free space. A first kind of those approaches uses the Biot-Savart law, to reduce the problem to a volume integral equation [2], [3], [4]. A second type of approaches combine FEM for the solution of the corresponding partial differential equation (PDE) inside the conductor with a boundary element method (BEM) based on the second Green's theorem to represent the field in the free space as an integral of the field values and its gradient over the surface of the conductor [5], [6]. In case of a thin skin-layer this approach reduces to a boundary integral equation [7]. On the other hand, there are approaches using the boundary impedance condition to approximate the field distribution in the conductor at small skin-depth in combination with a FEM solution in the free space [8].

Our approach is to reduce the problem to a boundary integral equation not only for the free space but also for the interior of the conductor that would be applicable regardless of the relative thickness of the skin-layer. This is possible for a conductor with uniform electric and magnetic properties when the field distribution inside the conductor is described by linear PDEs with constant coefficients admitting an analytic fundamental solution, *i.e.*, the Green's function. Advantage of this approach is a consideration of the conductor surface only. Thus, the dimensionality of the problem is reduced by one that renders this method particularly suited for the analysis of complicated geometrical configurations. On the other hand, this geometrical simplification comes at the price of an increased algebraic and numeric complexity due to the calculation of the axisymmetric Green's function. Similar approaches have already been considered for 2D [9], [10] and 3D [11] problems which both are considerably algebraically simpler than the axisymmetric problem considered here. There is an analytic solution for the Green's function for the 2D case and a point-source Green's function is used in the 3D case while there is no simple analytic solution for Green's function in the axisymmetric case. The axisymmetric case has been addressed by Fawzi *et al.* [19] who derived boundary integral equations for the transverse magnetic (TM) mode in terms of the azimuthal electrical and tangential magnetic fields in the full electrodynamic formulation including the displacement current. The same problem has been revisited in Refs. [20], [21] in a quasi-static approximation. Our approach differs from the previous ones by a more exact calculation of the

Green's function using a combination of analytic, asymptotic and numeric methods.

The paper is organized as follows. In Section II, problem formulation and basic equations are given. The boundary-integral equation derivation and the calculation of the Green's function for the azimuthal component of the vector potential is presented in Section III. In Section IV, we describe the numerical implementation of the method and give several application examples. Finally, summary and conclusions are given in Section V.

II. Problem Formulation and Basic Equations

Consider an axisymmetric body of a characteristic size R_0 at rest having a uniform electrical conductivity σ placed in an axisymmetric external ac magnetic field with induction $\boldsymbol{B}$ alternating harmonically in time with the angular frequency ω. Searching for magnetic and electric fields in terms of vector and scalar potentials as $\boldsymbol{A}(\boldsymbol{r},t) = \Re\left[\boldsymbol{A}(\boldsymbol{r})e^{i\omega t}\right]$ and $\Phi(\boldsymbol{r},t) = \Re\left[\Phi(\boldsymbol{r})e^{i\omega t}\right]$, where $\boldsymbol{A}(\boldsymbol{r})$ and $\Phi(\boldsymbol{r})$ are generally complex axisymmetric amplitudes, leads to the governing equation:

$$i\omega\boldsymbol{A} + \frac{1}{\mu_0\sigma}\boldsymbol{\nabla}\times\boldsymbol{\nabla}\times\boldsymbol{A} = -\boldsymbol{\nabla}\Phi. \tag{1}$$

In Eq. (1) the gradient of the scalar potential $\boldsymbol{\nabla}\Phi$ plays the role of a source term with respect to the vector potential. As it will be shown later, this source term can be used to specify an externally applied ac voltage to an axisymmetric coil system. For the following it is advantageous to use the transformation

$$\boldsymbol{A} = \boldsymbol{A}' + i\omega^{-1}\boldsymbol{\nabla}\Phi \tag{2}$$

that allows us to remove the source term from Eq. (1) by including it into the vector potential. Then the equation for $\boldsymbol{A}'$ satisfying the Coulomb gauge $\boldsymbol{\nabla}\cdot\boldsymbol{A}' = 0$ can be written as

$$\boldsymbol{\nabla}^2\boldsymbol{A}' - \lambda^2\boldsymbol{A}' = 0, \tag{3}$$

where $\lambda^2 = i\bar{\omega}$ with $\bar{\omega} = \mu_0\sigma\omega R_0^2$ being the dimensionless frequency. Henceforth all quantities and differential operators are supposed to be nondimensionalized by using the corresponding characteristic length and vector potential scales, R_0 and A_0, where the latter will be specified in the following for each particular problem. The advantage of Eq. (3) compared to its nonuniform counterpart (Eq. 1) is that the solution of the former can straightforwardly be written as a surface integral which is the aim of the next section.

III. Boundary-Integral Equation for the Vector Potential

Using second Green's vector theorem the solution of Eq. (3) satisfying the Coulomb gauge can be written as:

$$\begin{aligned}\boldsymbol{A}'(\boldsymbol{r}) = \frac{1}{4\pi}\int_S \big[&\boldsymbol{\nabla}G^\lambda(\boldsymbol{r}'-\boldsymbol{r})\times\boldsymbol{n}'\times\boldsymbol{A}'(\boldsymbol{r}') \\ &- \boldsymbol{\nabla}G^\lambda(\boldsymbol{r}'-\boldsymbol{r})\left(\boldsymbol{n}'\cdot\boldsymbol{A}'(\boldsymbol{r}')\right) \\ &- G^\lambda(\boldsymbol{r}'-\boldsymbol{r})\boldsymbol{n}'\times\boldsymbol{\nabla}\times\boldsymbol{A}'(\boldsymbol{r}')\big]\, d^2\boldsymbol{r}'\end{aligned} \tag{4}$$

where $G^\lambda(\boldsymbol{r}) = \frac{\exp(-\lambda|\boldsymbol{r}|)}{|\boldsymbol{r}|}$ is the Green's function of the scalar Helmholtz equation. Note that our approach here differs from that of Huang *et al.* [20] who uses a scalar counterpart of the second Green identity which is not correct in general but leads to the right result in the special case of an axisymmetric and purely azimuthal vector potential which satisfies the Coulomb gauge straightforwardly. To find $\boldsymbol{A}'$ at the point $\boldsymbol{r}$ inside the volume enclosed by surface S we need the values of both $\boldsymbol{A}'$ and $\boldsymbol{n}'\times\boldsymbol{\nabla}\times\boldsymbol{A}'$ on S. Usually both these values are unknown and two vector equations are needed to find them. The first of the equations is obtained by approaching the observation point $\boldsymbol{r}$ to the boundary S that results in:

$$\begin{aligned}\int_S \big[&\boldsymbol{\nabla}G^\lambda(\boldsymbol{r}'-\boldsymbol{r})\times\boldsymbol{n}'\times\boldsymbol{A}'(\boldsymbol{r}') - G^\lambda(\boldsymbol{r}'-\boldsymbol{r}) \\ &\boldsymbol{n}'\times\boldsymbol{\nabla}\times\boldsymbol{A}'(\boldsymbol{r}')\big]\, d^2\boldsymbol{r}' - 2\pi c(\boldsymbol{r})\boldsymbol{A}'(\boldsymbol{r}) = 0,\end{aligned} \tag{5}$$

where $c(\boldsymbol{r})$ is a geometrical parameter which is equal to unity for a smooth surface [12]. The second equation is obtained by considering the nonconducting space outside the body where the distribution of the vector potential is governed by a Laplace equation. The corresponding equation takes the form

$$\begin{aligned}\int_S \big[&\boldsymbol{\nabla}G^0(\boldsymbol{r}'-\boldsymbol{r})\times\boldsymbol{n}\times\boldsymbol{A} - G^0(\boldsymbol{r}'-\boldsymbol{r})\boldsymbol{n}\times\boldsymbol{\nabla}\times\boldsymbol{A}\big]d^2\boldsymbol{r}' \\ &+ 2\pi c(\boldsymbol{r})\boldsymbol{A}(\boldsymbol{r}) = 0,\end{aligned} \tag{6}$$

where the sign difference at the second term is because of $\boldsymbol{n}$ is directed inwards with respect to the region outside the body. Equation (5) can now be represented back in terms of the original vector potential $\boldsymbol{A}$ and the imposed gradient of the scalar potential by inverting the transformation given by Eq. (2): $\boldsymbol{A}' = \boldsymbol{A} - i\omega^{-1}\boldsymbol{\nabla}\Phi$.

In the following we focus on the case of a purely azimuthal and axisymmetric vector potential $\boldsymbol{A}(\boldsymbol{r}) = \boldsymbol{e}_\varphi A(r,z)$ depending only on the radius r and the axial coordinate z in a cylindrical system of coordinates. For the gradient of the scalar potential $\boldsymbol{\nabla}\Phi$ to be purely azimuthal and axisymmetric, Φ can be a function of the azimuthal angle φ only: $\Phi = \Phi(\varphi)$. Then $\boldsymbol{\nabla}\Phi = \boldsymbol{e}_\varphi\frac{1}{r}\frac{\partial\Phi}{\partial\varphi}$ with $\frac{\partial\Phi}{\partial\varphi} = \Phi_0 = const$ because of the axisymmetry. Further note that for axisymmetric bodies with simply connected shapes including the symmetry axis, Φ_0 must be zero for $\boldsymbol{\nabla}\Phi$ to be limited at the symmetry axis $r = 0$. However, Φ_0 may be nonzero for toroidal bodies which are not intersected by the symmetry axis. For such bodies, like coils, Φ_0 may be used to specify the externally applied voltage U driving the current as $\frac{\partial\Phi}{\partial\varphi} = \frac{U}{2\pi}$. Alternatively, Φ_0 may be determined in the course of solution when the total current rather than the voltage is specified on the coil. Note that our treatment of the source term is more mathematically rigorous compared to Ref. [20].

Substituting such a purely azimuthal vector potential into Eq. (6) and performing the integration along the azimuthal angle φ we obtain after some transformations an equation defining A outside the conducting body

$$\begin{aligned}A(\boldsymbol{r}) = -\frac{1}{4\pi}\int_L \Bigg[&\frac{\partial\left(r'A(\boldsymbol{r}')\right)}{\partial n'}G^0_\varphi(\boldsymbol{r},\boldsymbol{r}') \\ &- A(\boldsymbol{r}')\frac{\partial\left(r'G^0_\varphi(\boldsymbol{r},\boldsymbol{r}')\right)}{\partial n'}\Bigg]\, d\,|\boldsymbol{r}'|,\end{aligned} \tag{7}$$

where the integral is now evaluated along the contour L forming the conducting body of rotation. The Green's function

for the azimuthal component of the vector potential entering the above equation is

$$\begin{aligned} G^0_\varphi(\boldsymbol{r},\boldsymbol{r}') &= \boldsymbol{e}_\varphi \cdot \int_0^{2\pi} \boldsymbol{e}'_\varphi G^0(\boldsymbol{r}'-\boldsymbol{r})d\varphi' \\ &= \frac{2k}{\sqrt{r'r}}\int_0^{\pi/2} \frac{2\sin^2\varphi - 1}{\sqrt{1-k^2\sin^2\varphi}}d\varphi \\ &= \frac{4k}{\sqrt{r'r}}\left[\frac{K(k)-E(k)}{k^2} - \frac{K(k)}{2}\right], \end{aligned} \quad (8)$$

which is the vector potential of a circular current loop divided by r' [13] presented in terms of the complete elliptical integrals of the first and second kind, $K(k)$ and $E(k)$, respectively, of the modulus $k = 2\sqrt{\frac{r'r}{(r'+r)^2+(z'-z)^2}}$ [14]. Thus, the Green's function like its gradient for the azimuthal component of the Laplace equation is obtained analytically.

The azimuthal component of the vector potential inside the conducting body can be obtained in a similar way as outside by using the corresponding Green's function with $\lambda \neq 0$

$$\begin{aligned} A'(\boldsymbol{r}) = \frac{1}{4\pi}\int_L \Bigg[&\frac{\partial\left(r'A'(\boldsymbol{r}')\right)}{\partial n'} G^\lambda_\varphi(\boldsymbol{r},\boldsymbol{r}') \\ &- A'(\boldsymbol{r}')\frac{\partial\left(r'G^\lambda_\varphi(\boldsymbol{r},\boldsymbol{r}')\right)}{\partial n'}\Bigg] d\left|\boldsymbol{r}'\right|, \end{aligned} \quad (9)$$

where

$$\begin{aligned} G^\lambda_\varphi(\boldsymbol{r},\boldsymbol{r}') &= \boldsymbol{e}_\varphi \cdot \int_0^{2\pi} \boldsymbol{e}'_\varphi G^\lambda(\boldsymbol{r}'-\boldsymbol{r})d\varphi' \\ &= \frac{2k}{\sqrt{r'r}}\int_0^{\pi/2} \frac{2\sin^2\varphi - 1}{\sqrt{1-k^2\sin^2\varphi}} \\ &\quad \times \exp\left(-\kappa\sqrt{1-k^2\sin^2\varphi}\right)d\varphi, \end{aligned} \quad (10)$$

and $\kappa = 2\lambda\sqrt{r'r}/k$. In contrast to the previous case with $\lambda = 0$, the last integral cannot be evaluated analytically. For $|\kappa| \ll 1$, corresponding to low frequencies, the exponential function in (10) may be expanded into a power series of κ :

$$G^\lambda_\varphi(\boldsymbol{r},\boldsymbol{r}') = -\frac{2k}{\sqrt{r'r}}\sum_{n=0}^{\infty}\frac{(-\kappa)^n}{n!}\left(I_n + \frac{4}{n+1}I'_n\right), \quad (11)$$

where $I_n = \int_0^{\pi/2}\left(1-k^2\sin^2\varphi\right)^{\frac{n-1}{2}}d\varphi = \begin{cases} I^o_l, & n = 2l+1 \\ I^e_l, & n = 2l \end{cases}$, $l = 0,1,2,..$, and $I'_n = \frac{dI_{n+1}}{dk^2}$. For odd n the theory of elliptical integrals [15] yields the following recursion

$$I^o_{l+2} = \frac{2l+3}{2l+4}(2-k^2)I^o_{l+1} - \frac{l+1}{l+2}(1-k^2)I^o_l,$$

with $I^o_0 = \frac{\pi}{2}$ and $I^o_1 = \frac{\pi}{4}(2-k^2)$. Derivative of this recursion with respect to k^2 leads to a similar recursion for $I^{o'}_n$. Similarly, for even indices one obtains:

$$I^e_{l+2} = \frac{2l+2}{2l+3}(2-k^2)I^e_{l+1} - \frac{2l+1}{2l+3}(1-k^2)I^e_l,$$

with $I^e_0 = K(k)$ and $I^e_1 = E(k)$. Series (11) is summed until $\frac{|\kappa|^n}{n!} < 10^{-8}$ that ensures a relative error less than 10^{-5} for $|\kappa| < 5k^2$.

At high frequencies, when $|\kappa| \gg 1$, (10) is dominated by the maximum of the exponential function about the point $\varphi = \frac{\pi}{2}$ and it is possible to evaluate it asymptotically by the Laplace method [16]. Substitution of $\cos\varphi = t$ in Eq. (10) results in

$$G^\lambda_\varphi(\boldsymbol{r},\boldsymbol{r}') = \frac{2\beta}{\sqrt{r'r}}\int_0^1 \frac{\exp\left(-s\sqrt{1+\beta^2t^2}\right)}{\sqrt{1+\beta^2t^2}}\frac{\left(1-2t^2\right)}{\sqrt{1-t^2}}dt, \quad (12)$$

where $s = \kappa\sqrt{1-k^2}$ and $\beta = \frac{k}{\sqrt{1-k^2}}$. Since the dominating contribution in the above integral results from the vicinity of $t = 0$ we can expand $\frac{1}{\sqrt{1-t^2}} = \sum_{m=0}^{\infty}\frac{\Gamma(m+1/2)}{\sqrt{\pi}m!}t^{2m}$ and shift the upper limit of integration to infinity

$$\begin{aligned} G^\lambda_\varphi(\boldsymbol{r},\boldsymbol{r}') &= \frac{2}{\sqrt{r'r}}\int_0^\infty \exp\left(-s\cosh x\right)\left(1-2\left(\frac{\sinh x}{\beta}\right)^2\right) \\ &\quad \times \sum_{m=0}^{\infty}\frac{\Gamma(m+1/2)}{\sqrt{\pi}m!}\left(\frac{\sinh x}{\beta}\right)^{2m}dx \\ &= \frac{2}{\sqrt{r'r}}\sum_{m=0}^{\infty}\frac{\Gamma(m+1/2)}{\sqrt{\pi}m!\beta^{2m}}\left(I_m - \frac{2}{\beta^2}I_{m+1}\right), \end{aligned} \quad (13)$$

where we have made the additional substitution $t = \frac{\sinh x}{\beta}$. The integrals in the above relation

$$\begin{aligned} I_m &= \int_0^\infty \exp\left(-s\cosh x\right)\sinh^{2m}x dx \\ &= \frac{\Gamma(m+1/2)}{\sqrt{\pi}}\left(\frac{2}{s}\right)^m K_m(s), \end{aligned}$$

defined in terms of the modified Bessel function of the second kind of order m, $K_m(s)$, [14], can efficiently be calculated for $m > 1$ by the following recursion:

$$I_{m+1} = (2m+1)\left(2mI_m + (2m-1)I_{m-1}\right)/s^2.$$

The gradient of G^λ_φ can be found in a similar way by using the relation $\frac{dI_m}{ds} = -\frac{sI_{m+1}}{2m+1}$ which follows from the properties of Bessel functions [14].

There is an additional range of parameters where the power series solution given by Eq. (11) is not applicable because $|\kappa|$ is large, while the asymptotic approximation (13) does not work because k is small and the exponential function under the integral (10) varies weakly along the angle φ without having a pronounced maximum. In this case, one could expand the sub-integral function in Eq. (10) in a power series of k^2. As easy to see, this would result in the power series of $\sin^2\varphi$ which can in principle be integrated analytically term by term. On the other hand, such polynomials can efficiently be integrated by Gauss-Chebyshev-Lobatto quadratures. Thus, instead of expanding the integral (10) in a power series of small k^2 and then integrating analytically term by term, we apply a Gauss-Chebyshev-Lobatto quadrature [14] directly to the integral (12).

To summarize, three different approaches are used for the evaluation of the Green's function and its gradient for $\lambda \neq 0$ within the following parameter ranges defined in terms of k^2 and $|\kappa|$ which actually specify the integral in (10). First, for sufficiently small $|\kappa| \leq 5k^2$ we use the power series expansion (11). Second, for the intermediate range $5k^2 < |\kappa| < 35k^{-2}$ a

Gauss-Chebyshev-Lobatto quadrature with $M = 30 + 120k^4$ number of points is used where the number of points is increased as $k \to 1$ in order to ensure sufficient accuracy in the vicinity of the singularity at $k = 1$. In addition, for $k^2 > 0.98$ we subtract the singularity as the zero-frequency Green's function which can be integrated analytically whereas the rest is integrated numerically as described above. For $|\kappa| \geq 35k^{-2}$ the first five terms of the asymptotic series (13) are used. The ranges of applicability of different approximations and the number of the quadrature points are found numerically and they ensure the relative error of the Green's function and its gradient to be below 10^{-5} for $k \lesssim 0.999$.

Two coupled boundary-integral equations are obtained from Eqs. (7) and (9) by taking the observation point $\boldsymbol{r}$ to the surface contour L :

$$\int_L \left[\frac{\partial \Psi(\boldsymbol{r}')}{\partial n'} r G^0_\varphi(\boldsymbol{r}, \boldsymbol{r}') - \frac{\Psi(\boldsymbol{r}')}{r'} \frac{\partial \left(r' r G^0_\varphi(\boldsymbol{r}, \boldsymbol{r}') \right)}{\partial n'} \right] d|\boldsymbol{r}'| - 2\pi c(\boldsymbol{r}) \Psi(\boldsymbol{r}) = 0; \quad (14)$$

$$\int_L \left[\frac{\partial \Psi'(\boldsymbol{r}')}{\partial n'} r G^\lambda_\varphi(\boldsymbol{r}, \boldsymbol{r}') - \frac{\Psi'(\boldsymbol{r}')}{r'} \frac{\partial \left(r' r G^\lambda_\varphi(\boldsymbol{r}, \boldsymbol{r}') \right)}{\partial n'} \right] d|\boldsymbol{r}'| + 2\pi c(\boldsymbol{r}) \Psi'(\boldsymbol{r}) = 0, \quad (15)$$

where the unknown functions to be found along L are $\Psi(\boldsymbol{r}) = rA(\boldsymbol{r})$ and $\frac{\partial \Psi(\boldsymbol{r})}{\partial n}$, while $\Psi'(\boldsymbol{r}) = \Psi(\boldsymbol{r}) - i\bar{\omega}^{-1}\Phi_0$ for the interior involves an additional constant Φ_0 defining the azimuthal gradient of the electrostatic potential which, as discussed above, may be non-zero for the conductors not intersected by the symmetry axis. For such conductors the geometrical parameter in Eqs. (14, 15) can be determined as

$$c(\boldsymbol{r}) = \frac{1}{2\pi} \int_L \frac{1}{r'} \frac{\partial \left(r' r G^0_\varphi(\boldsymbol{r}, \boldsymbol{r}') \right)}{\partial n'} d|\boldsymbol{r}'|, \quad (16)$$

which follows from the requirement for Eq. (15) to be satisfied by a constant in the limit of $\lambda \to 0$ similarly to its PDE counterpart (3).

IV. Numerical implementation and examples of application

The system of two coupled boundary-integral Eqs. (14, 15) can be solved numerically by the boundary element method [12]. For this purpose each line L_k forming a closed surface of a part of the conducting body of rotation, which may be simply or multiply connected, is approximated by N rectilinear segments with endpoints pointed by radius vectors $\boldsymbol{r}_i$, $i = 1, .., N + 1$. The integrals in Eqs. (14-16) along each contour are replaced by the sums over the corresponding boundary elements where the integrals over each boundary element are approximated by four-point Gauss quadratures [17]. When the observation and integration points coincide there is a logarithmic singularity in the Green's function which is subtracted and integrated analytically over the corresponding element. In the simplest case, the unknown functions are considered to be constant within each element that results in $2N$ unknown quantities which are the constant values of $\Psi(\boldsymbol{r})$ and $\frac{\partial \Psi(\boldsymbol{r})}{\partial n}$ in each element. Upon evaluation of both Eqs. (14, 15) at the midpoint of each element we obtain a system of $2N$ complex linear equations. For a typical number of unknowns of about several hundreds this problem can straightforwardly be solved by an LU decomposition.

In the following, we consider two simple examples of application of the method. The first example is a conducting sphere of radius R_0 in a uniform external ac magnetic field with induction amplitude B_0. In this case, the contour encircling the whole free space in Eq. (14) may be considered to consist of two contours where L encloses the sphere while the second one encloses some remote inductor creating a uniform field with $\Psi_0(\boldsymbol{r}) = r^2/2$ that corresponds to the vector potential scaled by $A_0 = R_0 B_0$.

Thus Eq. (14) for the outer surface of the sphere takes the form

$$\int_L \left[\frac{\partial \Psi(\boldsymbol{r}')}{\partial n'} r G^0_\varphi(\boldsymbol{r}, \boldsymbol{r}') - \frac{\Psi(\boldsymbol{r}')}{r'} \frac{\partial \left(r' r G^0_\varphi(\boldsymbol{r}, \boldsymbol{r}') \right)}{\partial n'} \right] d|\boldsymbol{r}'| + 2\pi c(\boldsymbol{r}) \Psi(\boldsymbol{r}) = -4\pi \Psi_0(\boldsymbol{r}),$$

whereas the corresponding Eq. (15) for the inner surface remains unchanged. The distributions of $\Psi(\boldsymbol{r})$ and $\frac{\partial \Psi(\boldsymbol{r})}{\partial n}$ calculated with $N = 30$ constant surface elements are seen in Fig. 1 to be in good agreement with the corresponding analytical solutions [18]: $\Psi|_{|\boldsymbol{r}|=1} = \frac{3}{2} \frac{j_1(x)}{x j_0(x)} \sin^2(\theta)$ and $\frac{\partial \Psi}{\partial n}\big|_{|\boldsymbol{r}|=1} = \left(1 - \frac{1}{2} \frac{j_2(x)}{j_0(x)} \right) \sin^2(\theta)$, where $x = \sqrt{\bar{\omega}/i}$, θ is the poloidal angle, and $j_n(x)$ is the spherical Bessel function of order n [14].

An additional quantity which can be used for verification of the method is the total dissipated power defined in terms of dimensionless surface quantities as

$$P = \pi \bar{\omega} \int_L \Im \left[\frac{\partial \Psi}{\partial n} \frac{\Psi^*}{r} \right] d|\boldsymbol{r}|,$$

where the asterisk denotes the complex conjugate and the power is scaled by $P_0 = \frac{R_o B_0^2}{\sigma \mu_0^2}$. Comparison of numerical and exact solutions of total power for a sphere in a uniform ac magnetic field plotted in Fig. 2(a) shows that 30 constant boundary elements ensure a relative error below a few per cent for the dimensionless frequency up to 10^3. For comparison we show also the relative error of the solution resulting from purely numerical calculation of the Green's function and its gradient, as in Ref. [20], with 64 and 128 Gauss-Chebyshev-Lobatto quadrature points that results in a significantly lower accuracy at both low and high frequencies. As seen in Fig. 2(b), the accuracy decreases at high frequencies where a larger number of boundary elements is required. Note that the relatively slow convergence rate of about $\sim N^{-1}$ is due to the low accuracy of constant boundary elements used in this example.

As a next example we consider a model inductor consisting of two coaxial mirror-symmetric rings of trapezoidal cross-section as shown in Fig. 3 related to the crystal growth application by the floating zone technique [24]. The upper, primary, ring defined by the contour L_0 is connected to a power source supplying ac current $I = I_0 \cos(\omega t)$. The current in the lower, secondary, ring L_1, which is short-circuited through an additional impedance Z_2, is induced only by the magnetic field of the upper ring. In this case, we have two additional

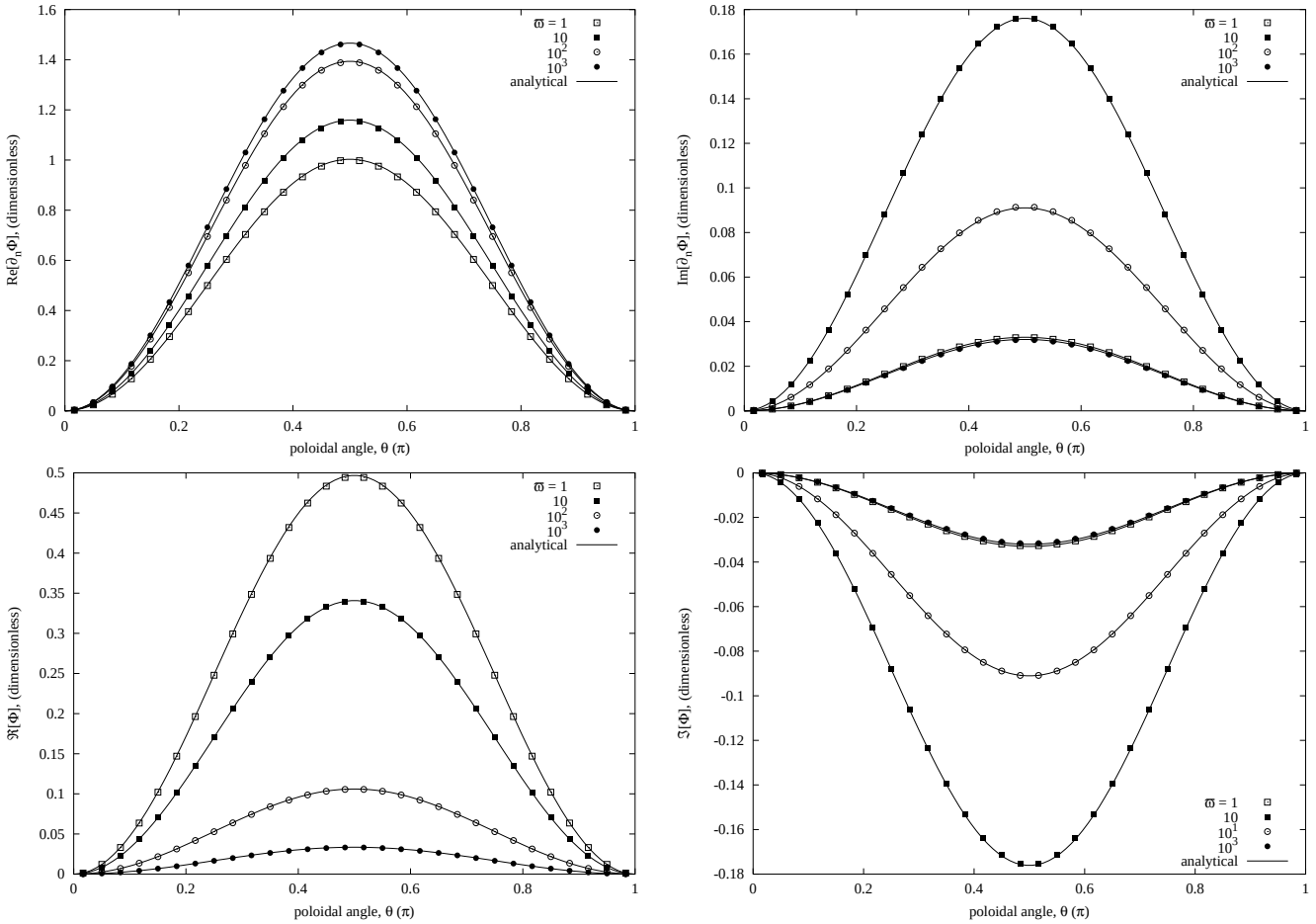

Fig. 1. Comparison of numerical (dots) and analytical (solid curves) solutions for a sphere in a uniform ac magnetic field: real (left) and imaginary (right) parts of Ψ (top) and $\frac{\partial \Psi}{\partial n}$ (bottom) at the surface of the sphere versus the poloidal angle for various dimensionless ac frequencies.

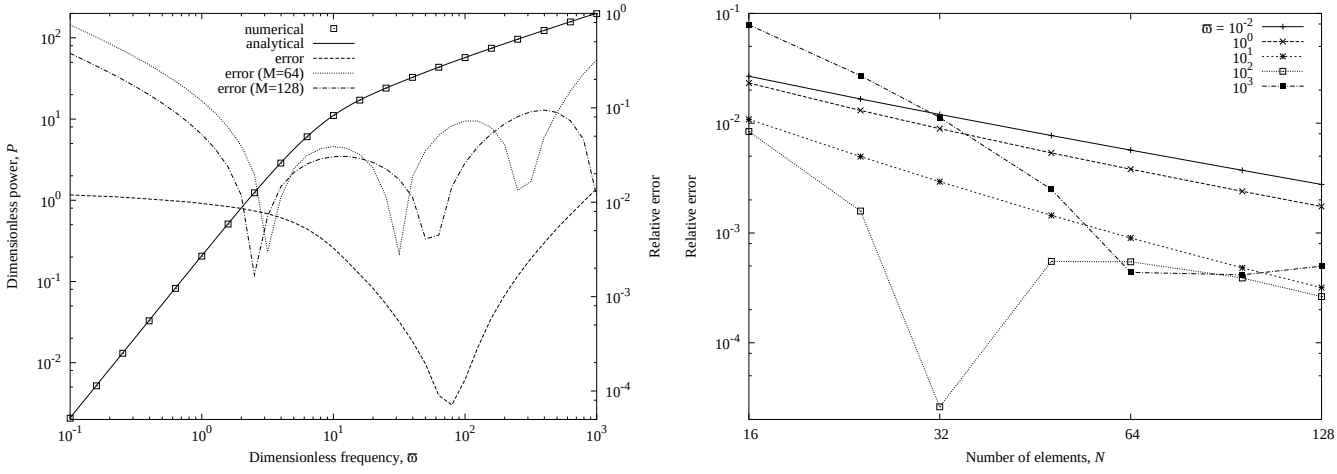

(a) (b)

Fig. 2. Comparison of the numerically obtained dimensionless dissipated power with the exact analytic solution for a sphere in a uniform ac field: power and the relative errors resulting from combined analytical/numerical and purely numerical calculations of the Green's function with $M = 64$ and $M = 128$ Gauss-Chebyshev-Lobatto quadrature points versus the dimensionless frequency for $N = 30$ boundary elements (a) and relative error versus the number of BEM at various dimensionless ac frequencies (b).

unknown quantities, the azimuthal gradients of the electrostatic potential Φ_0 and Φ_1 in the primary and secondary inductors. Respectively, we have two additional equations for the circuits of primary and secondary rings $I_0 = \int_{L_0} \frac{1}{r} \frac{\partial \Psi(\boldsymbol{r})}{\partial n} d|\boldsymbol{r}|$ and $\int_{L_1} \frac{1}{r} \frac{\partial \Psi(\boldsymbol{r})}{\partial n} d|\boldsymbol{r}| - 2\pi\Phi_1/Z_2 = 0$, which are discretized and solved as described above. Our goal here is to choose the additional impedance Z_2 so that to have the current induced in the secondary ring of the same amplitude but delayed in phase by 90 degrees with respect to the current in the primary ring. The corresponding magnetic flux lines calculated using 150 equally-sized boundary elements in each ring are plotted in Fig. 3 for various dimensionless frequencies. It has to be noted that the problem tends to be ill-conditioned at $\bar{\omega} = 0$ and, thus, special care is necessary for calculation of the geometrical parameter $c(\boldsymbol{r})$ defined by Eq. (16) in order to obtain accurate solutions at low frequencies $\bar{\omega} \ll 1$ which, however, are not very important for practical applications. The dimensionless impedances of primary and secondary circuits are plotted in Fig. 4(a) for the secondary current of the same amplitude but $\pi/2$ phase lag relative to the primary one. As seen, the results of the present approach are in good agreement with those of the boundary impedance condition (BIC) approximation which becomes applicable at sufficiently high frequencies ($\bar{\omega} > 10^2$). The results shown in Fig. 4(a) imply that for $\bar{\omega} \gtrsim 30$ the impedance of the secondary ring can be compensated by an additional impedance $Z_2 = R + \frac{1}{i\bar{\omega}C}$ containing active and capacitative components denoted by R and C, respectively. The relative amplitudes of the secondary current are plotted in Fig. 4(b) versus the dimensionless frequency for various impedances added in the circuit of the secondary coil. The solid curve corresponds to the short-circuited secondary ring. As seen, the capacitance determines the resonance frequency at which the amplitude of the secondary current attains a maximum while its phase becomes delayed by $\pi/2$ with respect to that of the primary current. The resistance is added to balance the amplitude of the secondary current with that of the primary one at the resonance frequency.

V. Summary and conclusions

We have presented a boundary-integral equation method for the calculation of poloidal axisymmetric magnetic fields applicable in a wide range of ac frequencies. The method is based on the vector potential formulation and uses Green's functions for Laplace and Helmholtz equations for the exterior and interior of conductors. Particular attention was paid to the calculation of Green's function for the Helmholtz equation which underlies our approach. In contrast to the Laplace equation, there is no simple analytic solution for the axisymmetric Green's function of the Helmholtz equation. Thus, the corresponding function as well as its gradient has to be calculated numerically that is done by three different approaches depending on the parameter range. For low and high dimensionless frequencies we use power series expansions in terms of elliptical integrals and asymptotic series in terms of modified Bessel functions, respectively. For the intermediate frequency range, Gauss-Chebyshev-Lobatto quadratures are used.

Our way of calculation of the Green's function differs considerably from previous approaches. Note that, on the one hand, our derivation of the axisymmetric Green's function is more straightforward and leads to considerably simpler analytic expressions compared to the Fourier series representation in terms of Bessel/Hankel and Legendre functions obtained by variable separation in spherical coordinates [21] or to the Fourier/Bessel integrals obtained by the corresponding integral transforms in the cylindrical coordinates [22], [23]. Fourier series and the corresponding integrals are computationally more expensive because they contain products of special functions of a varying argument whereas the power and asymptotic series in our case contain only a single special function of a fixed argument and varying order which can efficiently be calculated using recursion. Moreover, the selective calculation of the Green's function by either numerical quadratures, power or asymptotic series depending on its argument provides the best convergence in each parameter range and, thus, it is obviously more efficient numerically than a general Fourier series or corresponding integrals. On the other hand, the way in which we calculate the Green's function differs significantly from the approach of Huang *et al.* [20] who evaluate integral (10) numerically. Although before integration they subtract the Green's function for the Laplace equation in order to remove the singularity from the integrand, the discontinuities still remain in derivatives and deteriorate the accuracy of the numerical integration when the observation point approaches the contour of integration. Additional difficulties with numerical integration arise at high dimensionless frequencies when the exponential function in the integrand (10) decays in a fast and oscillatory way.

We avoid these problems by calculating the Green's function analytically in the form of power and asymptotic series for low and high frequencies, respectively.

The method was verified by comparison with the analytic solution for a sphere in a uniform ac magnetic field. In addition, the performance of the method was demonstrated for a composite model inductor supplied with a current of fixed amplitude and containing a secondary coil with an external circuit. In this case, the results were checked by comparison with an approximate solution obtained by the boundary impedance condition which becomes applicable at sufficiently high ac frequencies. The accuracy of the numerical solution deteriorates at very low frequencies where an increase of the number of boundary elements is necessary to obtain a smooth distribution of the magnetic field component shifted in phase by $\pi/2$ with respect to the applied potential.

The proposed method is well suited for the numerical calculation of axisymmetric poloidal magnetic field inductors of complicated geometrical configurations at intermediate ac frequencies because it requires only the surface but no spatial discretization.

References

[1] S. Gratkowski, T. Todaka, M. Enokizono, and R. Sikora, 'Asymptotic boundary conditions for the finite element modeling of axisymmetric electrical field problems,' *IEEE Trans. Magn.*, vol. 36(4), pp. 717–721, 2000.

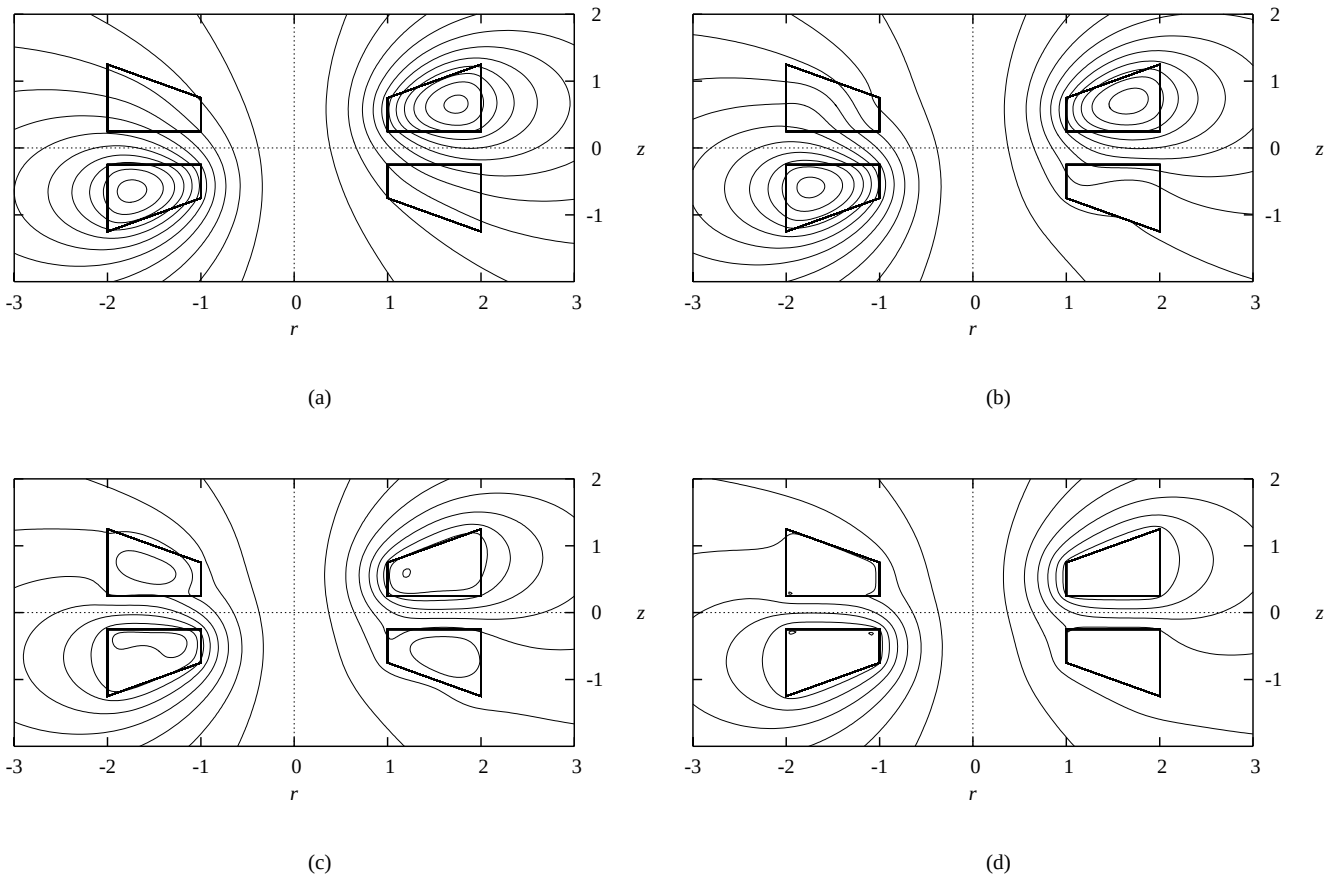

Fig. 3. Magnetic flux lines delivered by the surface-integral equations for a toroidal model inductor at various dimensionless ac frequencies $\bar{\omega}$: 1 (a); 10 (b); 10^2(c); 10^3(d). Right and left hand sides of each plot show the magnetic flux lines in phase and shifted by $\pi/2$ with respect to the current in the primary (upper) inductor that corresponds to the time instants when the current is at maximum and zero, respectively.

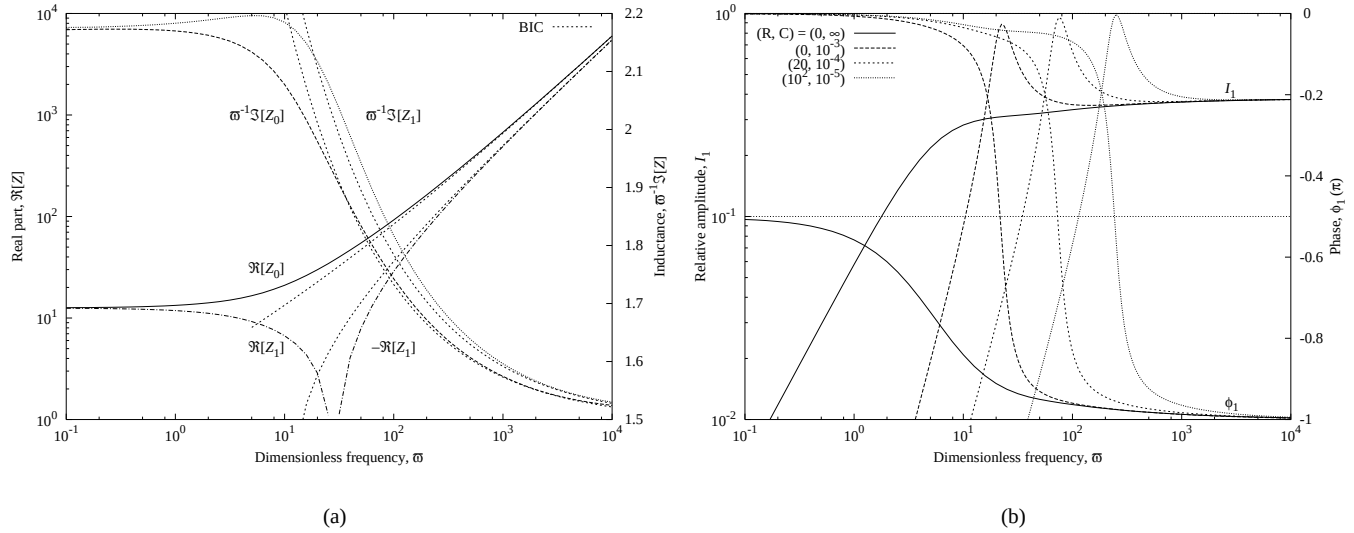

Fig. 4. Dimensionless impedances of primary (Z_0) and secondary (Z_1) rings of a model inductor supplied by the present method and boundary impedance condition (BIC) versus the dimensionless frequency $\bar{\omega}$ for the secondary current of same amplitude and $\pi/2$ phase lag with respect to the primary current (*a*). Relative amplitude and phase of the secondary current at various dimensionless values of active (R) and capacitive (C) impedance in the secondary circuit (*b*).

[2] G. Chitarin, M. Guarnieri, and A. Stella, 'An integral formulation for eddy current analyses in axisymmetric configurations,' *IEEE Trans. Magn.*, vol. 25(5), pp. 4330-4332, 1989.
[3] L. Kettunen and K. Forsman, 'Integral formulation for 3-D eddy current problems,' *IEE Proc.-Sci. Meas. Technol.*, 143(2), pp. 91–98, 1996.
[4] M. P. Volz and K. Mazuruk, 'Lorentz body force induced by travelling magnetic fields,' *Magnetohydrodynamics*, vol. 40, pp. 117–126, 2004.
[5] S. P. Song and B. Q. Li, 'A coupled boundary/finite element method for the computation of magnetically and electrostatically levitated droplet shapes,' *Int. J. Numer. Math. Engng.*, vol. 44, pp. 1055-1077, 1999.
[6] S. Börm and J. Ostrowski, 'Fast evaluation of boundary integral operators arising from an eddy current problem,' *J. Comp. Phys.*, vol. 193, pp. 67-85, 2003.
[7] H. Tsuboi, M. Tanaka, T. Misaki, and T. Naito, 'Three-dimensional analysis of eddy current and electromagnetic force in cold crucibles,' *IEEE Trans. Magn.*, vol. 30(5), pp. 3499–3502, 1994.
[8] B. Dumont and A. Gagnoud, '3D finite element method with impedance boundary condition for the modeling of molten metal shape in electromagnetic casting,' *IEEE Trans. Magn.*, vol. 36(4), pp. 1329-1332, 2000.
[9] J. M Schneider and S. J. Salon, "A boundary integral formulation of the eddy current problem," *IEEE Trans. Magn.*, vol. MAG-16, pp. 1086–1088, 1980.
[10] E. Basso-Ndjock and C. Broche, 'Two-dimensional field computations using boundary integral equations method for stationary and quasistationary problems with external current sources,' *IEEE Proc.*, 135, Pt. A, No 3, pp. 173-178, 1988.
[11] S. Kim, S. Ali, and J. White, 'A vector surface integral approach to computing inductances of general 3-D structures,' *IEEE MTT-S Digest*, pp. 1535-1538, 1993.
[12] C. A. Brebbia, J. C. F. Telles, and L. C. Wrobel, *Boundary element techniques*, New York: Springer, 1984.
[13] J. D. Jackson, *Classical Electrodynamics*, New York: Wiley, 1975.
[14] A. Abramowitz and I. A. Stegun, *Handbook of Mathematical Functions*, New York: Dover, 1965.
[15] G. A. Korn and T. M. Korn, *Mathematical handbook for scientists and engineers*, New York: McGraw-Hill, 1968.
[16] E. J. Hinch, *Perturbation Methods*, New York: Cambridge, 1991.
[17] W. H. Press *et al.*, *Numerical recipes in Fortran*, New York: Cambridge, 1992.
[18] W. R. Smythe, *Static and dynamic electricity*, New York: Hemisphere, 1989.
[19] T. H. Fawzi, K. H. Ali and P. E. Burke, "Boundary integral equations analysis of induction devices with rotational symmetry," *IEEE Trans. Magn.*, vol. MAG-19(1), pp. 36–44, 1983.
[20] Q. S. Huang, L. Krahenbuhl, A. Nicolas, "Numerical calculation of steady-state skin effect problems in axisymmetry," *IEEE Trans. Magn.*, vol. 24(1), pp. 201–204, 1988.
[21] A. Kost and M. Vix, "Calculation of eddy currents in a body of revolution by the boundary element method," In Boundary Elements X, Proc. of the 10th Internat. Conf., Southampton, pp. 517–533. Springer, 1988.
[22] C. V. Dodd and W. E. Deeds, "Analytical solutions to eddy-current probe-coil problems," *J. Appl. Phys.*, vol. 39(6), pp. 2829–2838, 1968.
[23] J. Yi, S. Lee, "Analytical solution for impedance change due to flaws in eddy current testing," *J. Nondestructive Evaluation*, vol. 4(3/4), pp. 197–202, 1984.
[24] R. Hermann, G. Behr, G. Gerbeth, J. Priede, H.-J. Uhlemann, F. Fischer, L. Schultz, "Magnetic field controlled FZ single crystal growth of intermetallic compounds," *J. Cryst. Growth* vol. 275, pp. 1533–1538, 2005.